Entwicklung und Implementierung eines FEM-basierten Ansatzes zur Berechnung der Wälzlagersteifigkeit

Inhalt: *Die Kenntnis der Lagersteifigkeiten ist in einem rotordynamischen System von besonderer Wichtigkeit, da sie einen wesentlichen Einfluss auf die Eigenfrequenzen des Gesamtsystems haben. Um einen sicheren Betrieb des Systems zu gewährleisten, sollten die kritischen Drehzahlen möglichst schnell durchfahren werden und die Betriebsdrehzahl möglichst weit von den Eigenfrequenzen entfernt sein. Da die auftretenden Schwingungen zudem verschiedene Geräusche sowie Schäden verursachen können, ist die Kenntnis der Lagersteifigkeit auch aus akustischer Sicht und für die Betrachtung der Lebensdauer von großer Bedeutung.*

Derzeit wird für die Berechnung der Lagersteifigkeit von Radialrillenkugellagern meist die Norm ISO/TS 16281 herangezogen, welche jedoch viele Aspekte, wie beispielsweise Lagerspiel oder Gehäusesteifigkeit und -spiel, ignoriert oder vereinfacht berücksichtigt. Daher wird in diesem Artikel eine neue Methodik vorgestellt, die realistische Steifigkeitswerte von Rillenkugellagern auf der Grundlage eines vereinfachten Finite-Elemente-Modells bestimmt, wobei die Elastizität der Lagerringe, die Lagerluft, der Gehäusesitz und die Gehäusesteifigkeit berücksichtigt werden.

Die vorgestellte Methodik wird implementiert und anhand von Referenzmodellen und Prüfstandversuchen validiert. Es zeigt sich, dass die Methode trotz des geringen Rechenaufwands eine sehr gute Übereinstimmung mit Referenzmodellen aufweist.

Stichwörter: *Finite Elemente Methode, Computer Aided Engineering, Maschinenelemente, Wälzlagersteifigkeit, Rotordynamische Systeme, Eigenfrequenzen*

1 Introduction

Many rotor dynamic applications are operated supercritically, i.e. their operating speed is above at least one natural frequency, which must be traversed from standstill. Wind turbines for example, have to go through frequent starts and stops due to changing wind conditions. To minimize the loads resulting from resonances, driving through these critical speed ranges should be done as fast as possible. In addition, the operating speed must not be too close to a natural frequency. The overestimation of the natural frequencies can lead to the total failure of the system. The design of rolling bearing rotor-dynamical systems thus requires the exact knowledge of their natural frequencies. Because the stiffness of the bearings has a significant influence on the vibration behaviour of the system and thus on its natural frequencies, its exact determination is considered important [1, 2, 3].

The dynamic modelling of powertrains often assumes linear bearing stiffness, e.g. in wind turbines [4]. However, rolling bearings have a non-linear stiffness behaviour, which is why the bearing stiffness at the operating point is of particular importance [5, 6].

The determination of the stiffness of rolling bearings is standardized in ISO/TS 16281 [7]. This standard represents a purely analytical approach and therefore requires a number of simplifications: The elasticity of the bearing rings and the connecting geometry is neglected, as well as the clearance fit between bearing outer ring and housing is not included in the calculation, which can lead to a deformation of the outer ring. In addition, the bearing internal clearance is taken into account only partially, which has particular influence on the load distribution of the rolling elements. Due to the bearing's internal clearance only a few rolling elements are in contact at low load. Only after an ovalization of rings or deformation of the rolling elements more rolling elements can come into contact. The factors mentioned above indeed have a major influence on the lowering of the bearing under load and the resulting bearing stiffness [1, 6]. The standard ISO/TS 16281 is also used to determine the rolling bearing stiffness in calculation programs such as KISSsoft [8] or LAGER2 [9].

For the determination of stiffness parameters, which do not have the above restrictions, there are currently two main procedures available. On the one hand, the stiffness values can be determined by time consuming physical experiments (test bench), which often involves high costs. The second approach is to determine the stiffness of the bearings by means of numerical methods. Here, the most common approach is a Finite Element analysis, in which the bearing and the housing are fully modelled using three-dimensional volume elements, as in [6] or [10]. It should be noted that automatic model generation is very difficult for different types of bearings. Furthermore, full Finite Element models require very long computation times and often have convergence difficulties, which in turn makes model automation problematic. For this reason, a new approach is needed which allows an automated stiffness calculation of bearings taking into account elastic bearing rings, the connecting geometry (in particular the housing clearance fit) and the bearing internal clearance. This article presents and discusses a fully automated approach employing a simplified calculation method based on the Finite Element method to evaluate the radial rolling bearing stiffness under realistic conditions.

2 Development of a simplified calculation method

To develop a simplified calculation method for rolling bearings, first the whole bearing system is divided into sub-assemblies, as seen in Fig. 1. All of these components have to be included in the substitute model to obtain realistic stiffness values. [11]

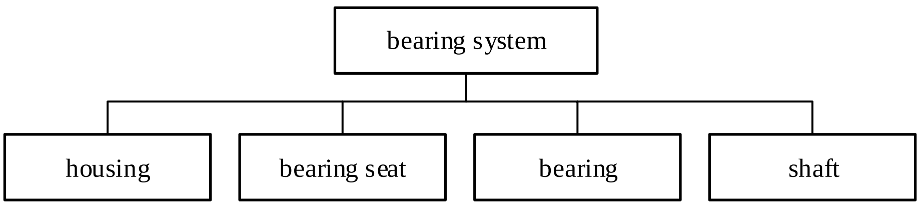

Figure 1: Sub-assemblies of a bearing system [11]

As mentioned in the introduction, a fully modelled and meshed Finite Element assembly, consisting of the three-dimensional meshed (hexahedron/tetrahedron) rings and rolling elements (see Fig. 2) is capable of representing the whole bearing system and its stiffness.

The benefits of this method are the exact representation of the rolling bearing geometry (e.g. bearing internal clearance and housing clearance fit). On the downside, the automatic generation of the three-dimensional meshes of the rings and rolling elements is quite complex. Furthermore, the meshes must be very fine to accurately model the Hertzian contact between the rings and the rolling elements, which leads to very high computation times. Besides that, the model is very sensitive towards contact properties, which can complicate the automation of the stiffness calculation. [6]

For this reason, an attempt was made by [11] to develop a substitute model which does not possess the disadvantages explained. As described, the Hertzian contact between the bearing rings and the rolling elements requires a very fine mesh at the contact areas and a contact algorithm, which can lead to high computing times and convergence problems. Therefore, in the substitute model proposed in [11], the rolling elements are replaced by rod elements which connect the inner and the outer ring and have the same stiffness behaviour as the rolling elements (see Fig. 3). Due to this simplification, the mesh of the bearing rings can be significantly more coarse and the contact calculation between the rolling elements and the bearing rings can be omitted.

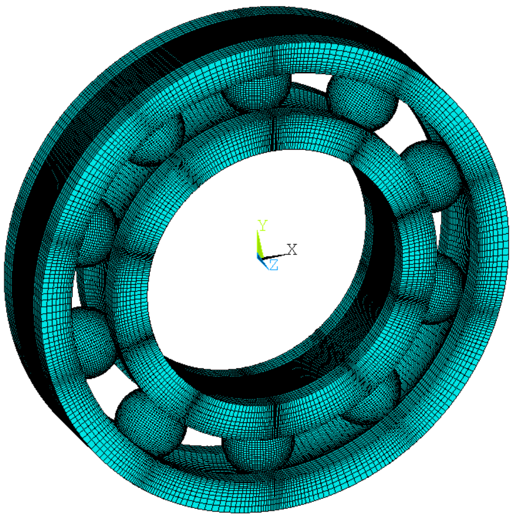

Figure 2: Full Finite Element model of a deep groove ball bearing (without housing)

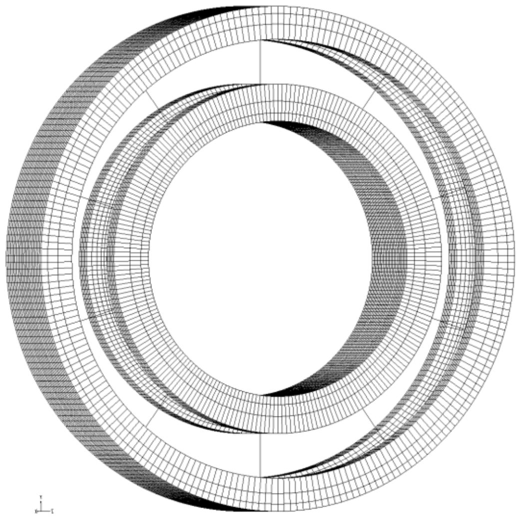

Figure 3: Substitute model of a deep groove ball bearing (without housing); rolling elements substituted by rods

Because the very rigid shaft it is expected to have little effect on the stiffness of the bearing system, the shaft is not explicitly modelled but replaced by a rigid coupling element which couples a central shaft reference node to the inner ring of the bearing. In order to model correctly all the relevant effects of the bearing seat, the housing is explicitly modelled by volume elements. By defining a contact condition between the outer ring of the bearing and the bore surface, the housing fit can be modelled realistically.

3 Implementation of the calculation algorithm

After evaluating a modelling strategy with a good compromise between accuracy and calculation speed, this strategy was implemented in an automated calculation tool [6]. The implementation details are discussed in this chapter.

3.1 Calculation methods

The calculation tool implements two different methods of the assembly generation. In the first calculation mode (CM 1, see Fig. 4) a structured FE mesh of the rolling bearing assembly is automatically created. The inner and outer rings are represented by linear hexahedron elements with eight nodes, which are created by the rotation of a two dimensional structured quadrilateral cross section mesh of the rings [12, 13]. The rolling elements are modelled with one rod per rolling element, which connect the inner and outer ring. There is no explicit modelling of the shaft, instead there is one rigid coupling element, which connects one reference point in the centre of the bearing with the nodes at the inner surface of the inner ring. The load will be applied at this reference node. The whole outer surface of the outer ring is fixed in all directions. This model is used to calculate the bearing stiffness without the influence of the housing.

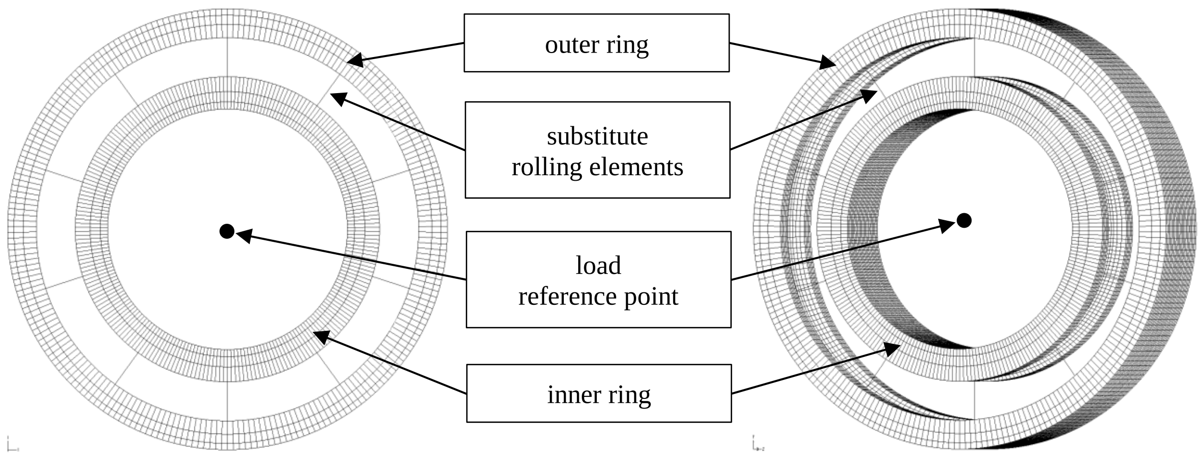

Figure 4: Bearing substitute model in calculation mode 1 (CM 1; without housing)

Calculation mode two (CM 2, see Fig. 5) creates an additional mesh for a ring-shaped housing. The housing and the rolling bearing are combined into an assembly. Furthermore, a contact definition is set up between the two parts. In this calculation mode, the load is also applied at the reference node in the centre of the bearing, but instead of clamping the outer ring surface, the outer surface of the housing is fixed in all directions.

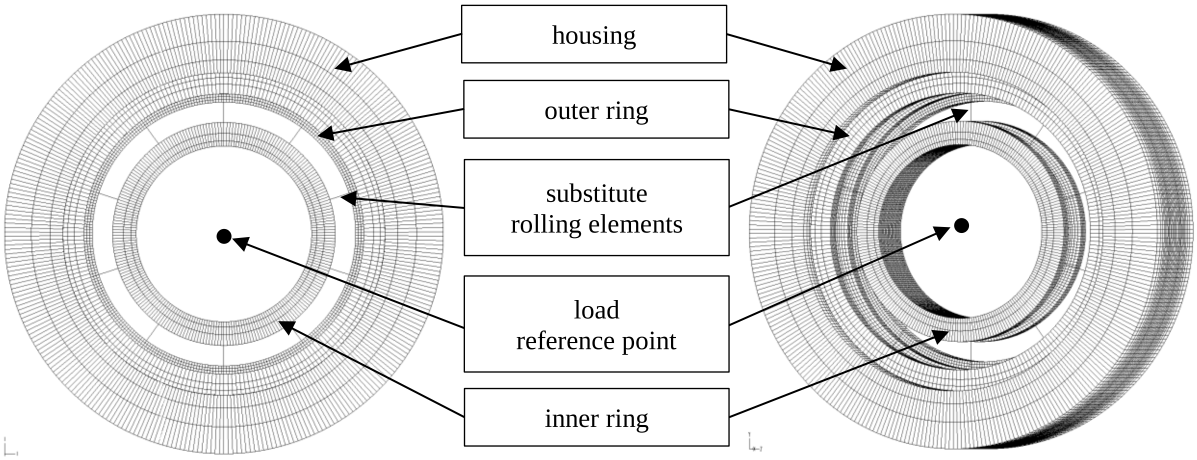

Figure 5: Bearing substitute model in calculation mode 2 (CM 2; with housing)

All necessary geometric parameters for creating the FE model are supplied in an input text file:

Deep Groove Ball Bearing:

- Outer diameter D
- Bore diameter d
- Shoulder diameters D_1 and d_1
- Raceway diameters D_2 and d_2
- Rolling element diameter D_r
- Bearing width B
- Outer and inner osculation κ_o and κ_i

Ring Housing:

- Diameter D_0
- Shoulder diameter D_{aG}
- Width B_0
- Clearance fit

The bearing internal clearance and housing clearance fit are explicitly modelled in the assembly.

3.2 Hertzian contact between bearing rings and rolling elements

The rods between the two bearing rings must have a nonlinear behaviour to mimic the real Hertzian contact conditions. In addition, an algorithm has to be developed to imitate the behaviour caused by the bearing internal clearance discussed earlier. This nonlinear behaviour can be realized by applying the load iteratively to the whole bearing system and by calculating the deformation of the bearing in every substep. After each step the length of each rod is determined. Based on the rod length, a new calculated Young's modulus is assigned to each rod. The relation between rod stiffness as a function of their corresponding length is calculated by the Hertzian contact equations.

The relation between the contact force F and the rolling element deformation u is given in Eq. (1) [7]:

$$F(u) = c_p \, u^{3/2} \tag{1}$$

The spring constant c_p is a geometry-based value, which can be calculated for each bearing [7]. To obtain the stiffness of the contact point, F can be differentiated with respect to u, which leads to Eq. (2):

$$c(u) = \frac{dF}{du} = \frac{3}{2} c_p \sqrt{u} \tag{2}$$

Thus, the Young's modulus of each rod can be calculated by using Eq. (3), where l describes the length and A the cross section of the rod which is set to a constant factor:

$$E = \frac{cl}{A} \tag{3}$$

To mimic the behaviour, which is caused by the bearing internal clearance, the cross section A of all rods that are larger than the rolling element diameter D_r is set to zero, which leads to a Young's modulus of $E = 0$.

The calculated stiffness has to be adjusted, because the Hertzian contact contains the stiffness of the whole contact, which includes the inner ring, the rolling element and the outer ring. This is equivalent to three springs in series. Because of the elastic inner and outer ring in this model, the rod has only to mimic the stiffness of the rolling element. To achieve this, the calculated stiffness is adjusted accordingly via a constant factor [14].

3.3 Housing fit tolerance consideration

Another critical criterion to be considered is the clearance fit between outer bearing ring and housing. For realistic modelling, the clearance fit is taken into account when generating the meshes of the ring and the housing. Thus, an ovalization of the outer ring is possible, which changes the load distribution of the rolling elements. To achieve this, a contact definition has to be defined. In general, three different contact methods are available:

1. Tied contact: constrained surfaces tied together,
2. Frictionless contact: constrained surfaces can separate and slip without friction,
3. Friction contact: constrained surfaces can separate and slip with friction.

A friction contact would lead to the most realistic results but is very computationally expensive. Due to the expected low friction coefficients between the bearing and the housing and the goal of achieving a fast calculation method, a frictionless contact method is used in the described approach. Furthermore, there is no rotation of the ring possible, so the acting contact forces are mostly normal forces. In this case, the frictionless contact yields sufficiently accurate results.

3.4 Calculation process

The whole calculation process is displayed in the following figure:

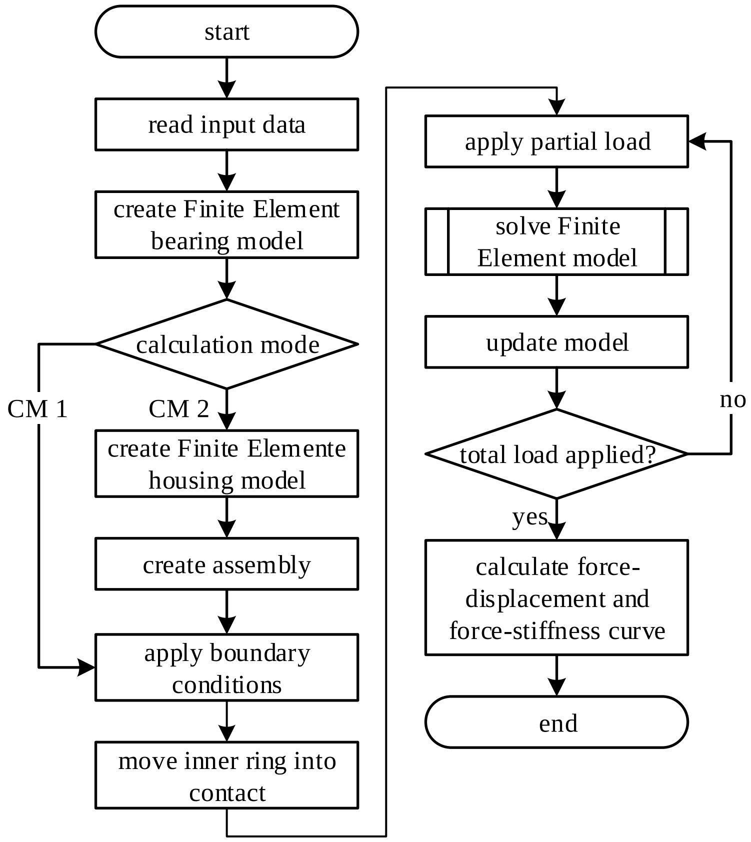

Figure 6: Calculation process of the substitute model

The program works as follows: After reading the input file and calculating the c_p spring constant of the bearing, the bearing model is created. This step consists of creating the hexahedron meshes for the bearing rings, integrating the rod elements for substituting the rolling elements and defining the material properties for the rings and each rod. Furthermore, the rigid coupling is integrated into the calculation model to represent the shaft.

If CM 2 is used (calculation with housing), an additional hexahedron mesh representing the housing is automatically created. The housing is integrated into the rolling bearing assembly and is moved towards the load direction until the bearing and the housing come into contact. Additionally, the material properties of the housing are defined.

In the next step, the necessary boundary conditions for the calculation are defined. As stated in chapter 3.1, in CM 1 the whole outer surface of the outer ring is fixed in x-, y- and z-direction. In CM 2 there are no boundary conditions applied to the outer ring, because it seats in the housing, instead the outer surface of the housing is fixed. The load steps are applied to the reference point in the centre of the inner ring. Furthermore, there are additional boundary conditions at the reference node to ensure a numerically stable behaviour:

- Locking the displacement in axial direction,
- Locking the displacement in the second radial direction,
- Locking all rotation degrees of freedom.

Besides that, it must be observed that the outer ring of the bearing is statically indeterminate, because it is only connected via rod elements, which cannot transmit torque. Therefore, a rotation of the outer ring around the shaft axis is possible. To prevent this behaviour, the displacement of the uppermost rod node in load direction is locked in the perpendicular direction of the load direction. This serves only numerical purposes and has no stiffness influence.

Subsequently the inner ring is moved about the bearing internal clearance in load direction to ensure that at least one "rolling element" respectively rod is in contact. Because Eq. (2) evaluates to zero when the displacement $u = 0$, the inner ring is moved an additional small initial displacement. Thus, at least one rod is transmitting force in the first load step.

Now the main loop of the calculation program starts. The total load is divided into smaller load steps, which are gradually applied to the shaft reference node in the Finite Element model. Due to this, the nonlinear rod behaviour can be solved with linear Finite Element analyses. The number of load steps and their subdivision (linear/logarithmic) can be defined in the input file. In each step the Young's modulus of the rods is being re-calculated: First, a cross section of zero is defined for all rods which are longer than the rolling element diameter, because at these positions there would be no contact between the rolling elements and the rings. With Eq. (3) this leads to a Young's modulus of zero. For all other rods, the displacement/compression u is calculated. Knowing u, the Young's modulus E can be derived from Eq. (2) and Eq. (3). After solving the model, the displacements are transferred to the next step. This process will be repeated until the total load is applied to the model.

Finally, the discrete force-displacement points of all load steps are fitted through the least-squares-method with the trial function $u(F) = aF^b + cF + d$. To improve the convergence of this nonlinear optimization problem, the default values of the parameters were defined as follows: $a = 0$, $b = 2/3$, $c = 0$, $d = \text{bearing internal clearance}$.

This function is then analytically derived and inverted (see Eq. (4)), which leads to a stiffness function of the whole bearing system in respect to its load:

$$c(F) = \left(\frac{du(F)}{dF}\right)^{-1} \tag{4}$$

4 Validation of the calculation method

In the following the results of the developed modelling strategy is to be investigated and validated by the results of the full FE model and the test bench [6]. For the comparisons, a bearing of the type 6212 from the bearing manufacture Schaeffler is used. The bearing has a bore diameter of $d = 60\ \text{mm}$, an outer diameter of $D = 110\ \text{mm}$ and a static load rating of $C_0 = 36\ \text{kN}$ [15]. The maximum applied load is $7.2\ \text{kN}$ ($C_0/P = 5$).

In Fig. 7 the force-displacement plot of the proposed substitute model is compared to that of a full FE model. A validation against the test bench is not possible for CM 1 due to the fact that bench tests cannot be accomplished without a housing.

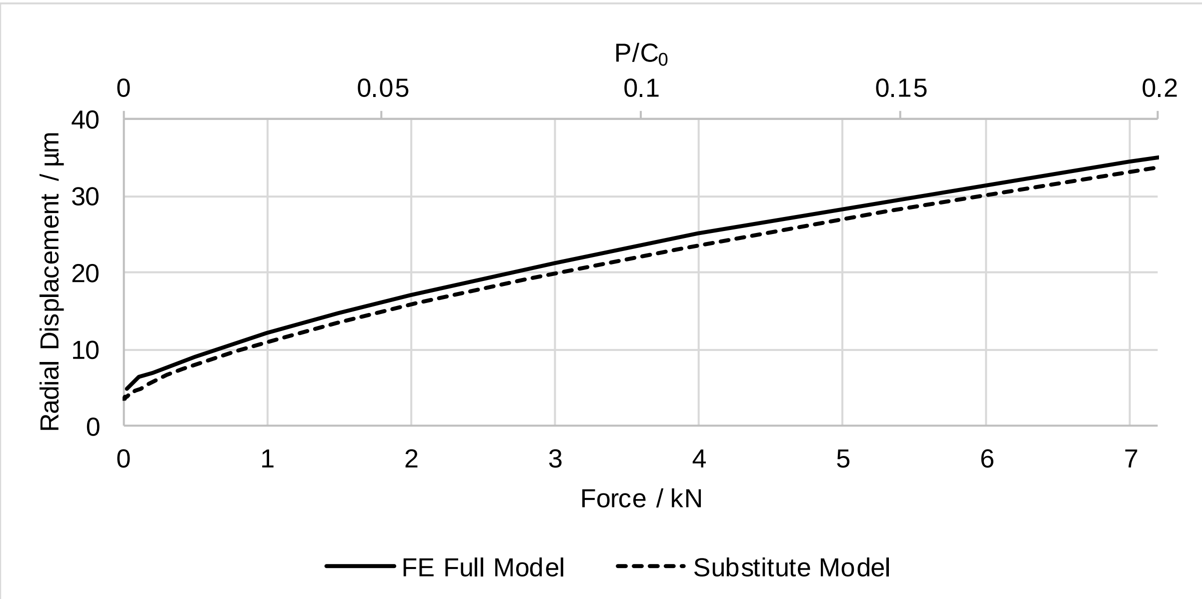

Figure 7: Radial displacement over force (CM 1: no housing) for the deep groove ball bearing 6212

The results of the full FE model and the substitute model show a very good match. A nearly constant offset of less than $2\ \mu m$ is apparent, which has no influence on the result due to the differentiation of the curves to achieve the stiffness. A possible reason for this offset is for example the unavoidable contact penetration of the rolling element and ring meshes in the full FE model, which does not occur in the discussed substitute model. The radial stiffness curves are shown in Fig. 8.

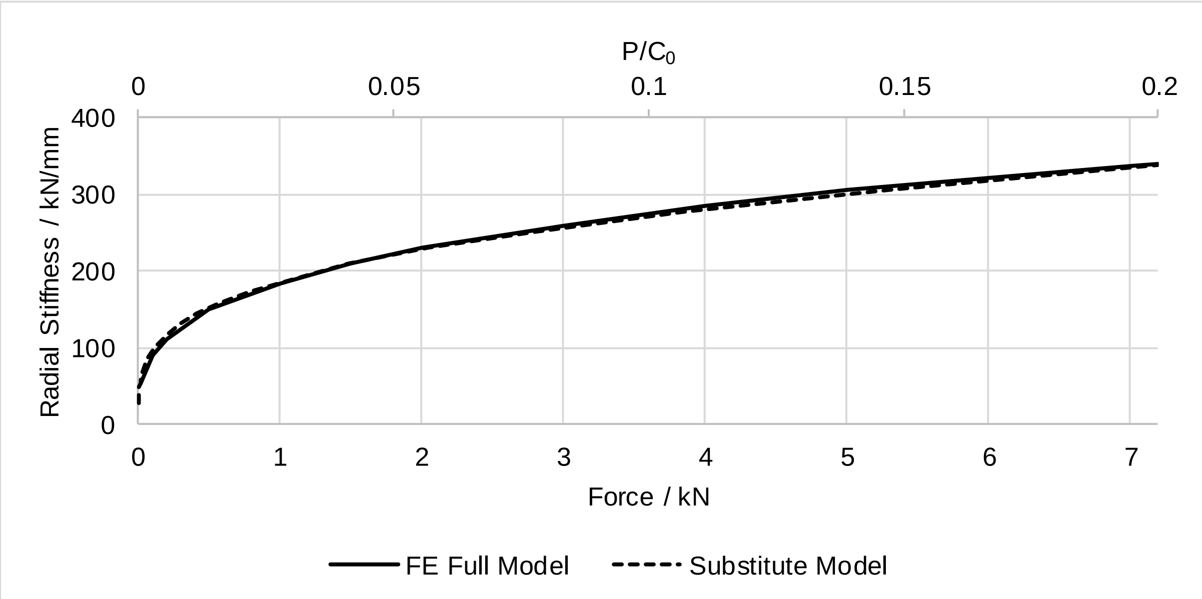

Figure 8: Radial stiffness over force (CM 1: no housing) for the deep groove ball bearing 6212

There is no noticeable deviation (below 2% in the load range from $0.5\ \mathrm{kN}$ to $7.2\ \mathrm{kN}$) and the curves are almost congruent. Thus, it should be noted that for a fixed outer ring the substitute model provides very good results in comparison to the full FE model. The advantage of calculating the bearing system stiffness with the substitute model instead of analytical formulas is that the influence of the bearing internal clearance and hence the different rolling element load distribution is taken into account.

In the following, the results of the substitute model against the full FE model and the test bench results are to be validated taking into account the housing and thus the housing clearance fit (CM 2). For this purpose, the displacement and stiffness over bearing load plots for a housing clearance of $3\ \mu m$ are compared in Fig. 9 and Fig. 10.

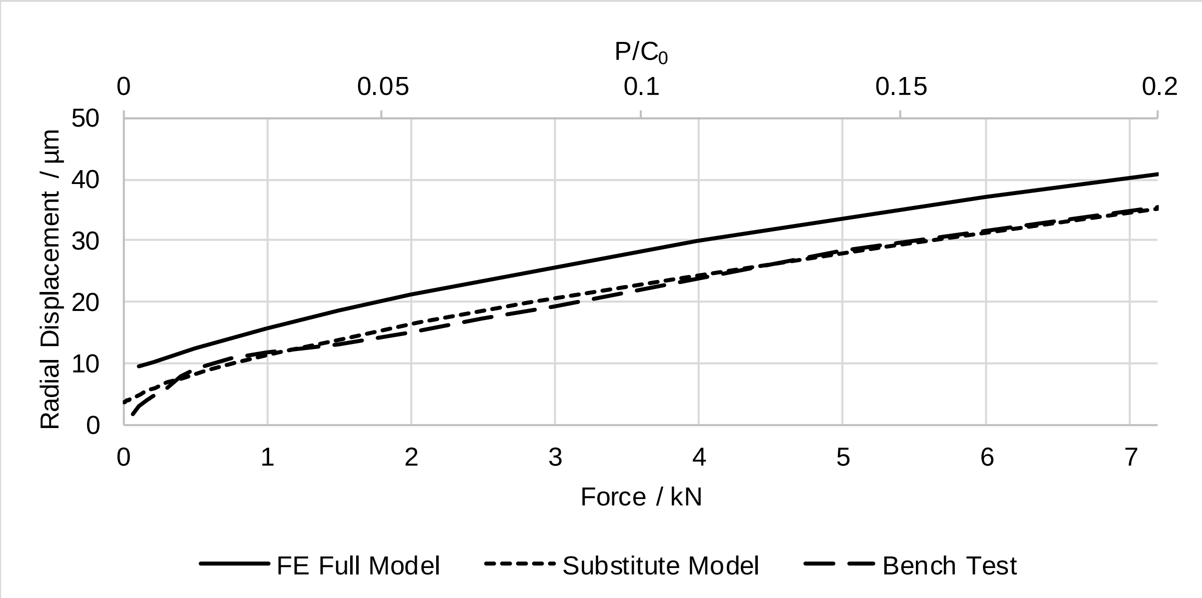

Figure 9: Radial displacement over force (CM 2: $3\ \mu\mathrm{m}$ housing clearance fit) for the deep groove ball bearing 6212

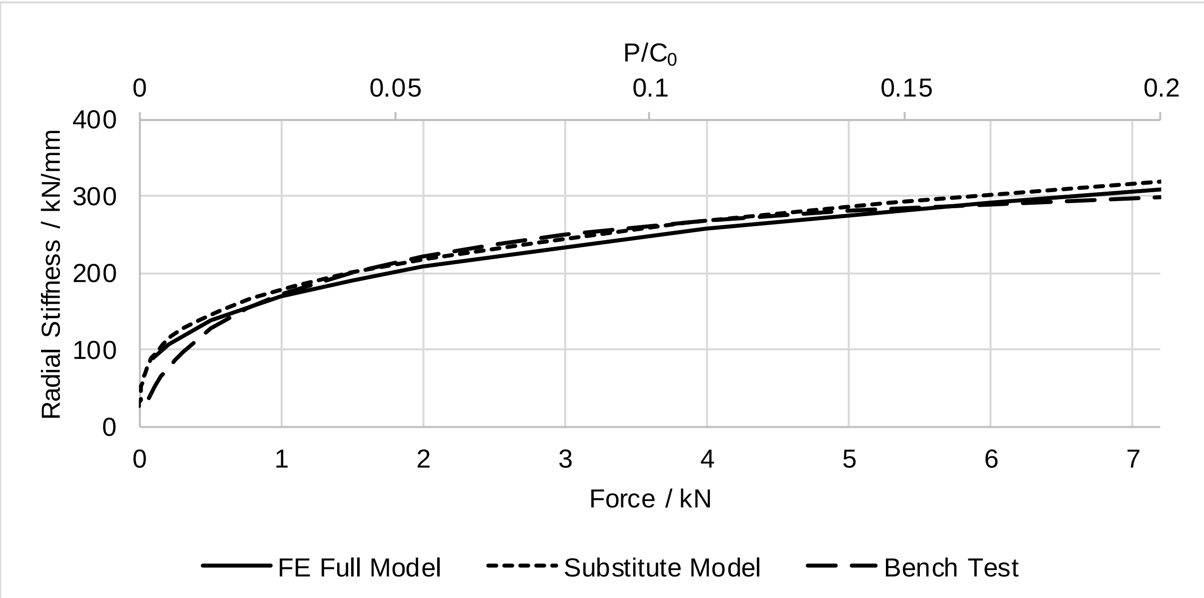

Figure 10: Radial stiffness over force (CM 2: $3\ \mu\mathrm{m}$ housing clearance fit) for the deep groove ball bearing 6212

This comparison also shows the good agreement between the substitute model, the full FE model and the test bench. The difference in the displacement over force plots is merely a relatively constant offset, which has as stated before no effect on the stiffness curves. The maximum deviation of the stiffness curves of the two simulation models is at a maximum of 5.3% in the relevant load range from $0.5\ \mathrm{kN}$ to $7.2\ \mathrm{kN}$. Therefore a high accuracy of the substitute model can be confirmed for this calculation model as well.

5 Conclusion

In this paper, a methodology for the automatic calculation of the bearing stiffness was presented and its implementation described. The calculation tool generates a Finite Element model based on an input text file. In the next step the load is iteratively applied to the model, thus simulating the deformation and the associated rigidity of the bearing. This new approach takes into account many effects that are commonly not considered in state-of-the-art methods.

The method was validated against a full Finite Element model and bench tests. The compared force-displacement and force-stiffness values yield a very good agreement of all approaches. Thus, this method can be used in the future design of rotor-dynamical systems to ensure its safe operation. Further research will investigate how the presented approach can be applied to other bearing types and how combined load cases can be taken into account.

6 Acknowledgement

This work has been supported by the Forschungsvereinigung Antriebstechnik e.V. (FVA) and the Industrielle Gemeinschaftsforschung (IGF) in Germany as part of the project FVA 747 I respectively IGF 18735 N.

References

[1] Dresig, H.; Holzweißig, F.: *Maschinendynamik*. 10th edition, Berlin: Springer, 2011.

[2] Steinhilper, W.; Röper, R.: *Maschinen- und Konstruktionselemente 3*, 2nd edition, Berlin: Springer, 1996.

[3] Schlecht, B.; Breslau, G.; Ulrich, C.: *Zur Modellbildung und Simulation von Zylinderrollenlagern*. Proceedings of the Dresdner Maschinenelemente Kolloquium, pp. 343-362, 2017.

[4] Srikanth, P.; Sekhar, AS.: *Dynamic analysis of wind turbine drive train subjected to nonstationary wind load excitation*. Proceedings of the Institution of Mechanical Engineers, Part C: Journal of Mechanical Engineering Science, Vol. 229, No. 3, pp. 429-446, 2014.

[5] Raabe, M: *Moderne Wellenberechnung unter Berücksichtigung nichtlinearer Effekte aus der Wälzlagerinnengeometrie.* Proceedings of the Dresdner Maschinenelemente Kolloquium, pp. 241-250, 2007.

[6] Glamsch, J.; Sebteini, S.; Rieg, F.; Sauer, B.: *Bestimmung der Wälzlagersteifigkeit unter Berücksichtigung der Innen- und Außenringelastizität und des Passungsspiels für die Rotordynamikauslegung*. Final Report Industrielle Gemeinschaftsforschung IGF 18735 N, 2017.

[7] Norm ISO/TS 16281:2008-06. *Rolling bearings - Methods for calculating the modified reference rating life for universally loaded bearings.*

[8] KISSsoft AG: *Handbook KISSsoft*. Version 03/2017A.

[9] Schleich, T.; Otto, M.: *Lebensdauer-Industriegetriebe-Wälzlager III - Erweiterung der FVA Programme RIKOR und LAGER2 zur Bestimmung der Lebensdauer von Wälzlagern in Industriegetrieben*. Final Report Forschungsvereinigung Antriebstechnik e.V. FVA 364 III, 2011.

[10] Guo, Y.; Parker, R.: *Stiffness matrix calculation of rolling element bearings using a finite element/contact mechanics model*. Mechanism and Machine Theory, Vol. 51, pp. 32-45, 2012.

[11] Braun, M.; Sebteini, S.; Rieg, F.; Sauer, B.: *Bestimmung der Wälzlagersteifigkeit unter Berücksichtigung der Innen- und Außenringelastizität und des Passungsspiels für die Rotordynamikauslegung*, Mid-Term Report Industrielle Gemeinschaftsforschung IGF 18735 N, 2016.

[12] Viebahn, F.: *Systematische Untersuchung der Anwendbarkeit der Finite-Elemente-Analyse zur Abbildung des Wälzlagerwanderns mittels der statistischen Versuchsplanung (PhD-Thesis)*. Aachen: Shaker Verlag, 2018.

[13] Neidnicht, M.: *Numerisches Abbildungsvermögen als Maßgabe zuverlässiger Finite Elemente-Netzgenerierung (PhD-Thesis).* Aachen: Shaker Verlag, 2013.

[14] Brändlein, J.; Eschmann, P.; Hasbargen L.; Weigand, K.: *Die Wälzlagerpraxis - Handbuch für die Berechnung und Gestaltung von Lagerungen*. 3rd edition. Mainz: Vereinigte Fachverlage GmbH, 1998.

[15] Schaeffler: *Wälzlager*. 1st edition. Herzogenaurach: Schaeffler KG, 2008.